Orsang Man: a robust Homo sapiens in Central India with Asian Homo erectus features

Anne Dambricourt-Malassé, Rachna Raj, Samit Shah

Orsang Man: a robust *Homo sapiens* in Central India with Asian *Homo erectus* features

A. Dambricourt Malassé[1]*, Rachna Raj[2], S. Shah[3]

1. UMR 7194 CNRS, Department of Prehistory, National Museum of Natural History, Institut de Paléontologie Humaine, Paris, France.
2. Department of Geology, The Maharaja Sayajirao University of Baroda, Vadodara, India.
3. Aster Diagnostic & Therapeutic Radiology Services, Vadodara, India.

*Corresponding author. E-mail address: iphadm@mnhn.fr

Abstract
A *Homo sapiens* calvarium recovered in a fluvial deposit of the Orsang River give evidence of genetic continuity between late Asian *Homo erectus* suggesting an Asian "like-cromagnoid" stadium in the evolutionary process. IRSL dating of the host sediments provided an age ranging from 50 to 30 ka. The interesting features observed are a well-developed asteriac process or gracile *torus angularis*, a well-developed supramastoid crest, a very broad frontal sinus in the glabellar area, the greatest width located in the lower part of the cranium. CT-scan shows no pneumatization of the mastoid process as in *Homo erectus*, but two temporal bosses. The study establishes that in the absence of new contradictory data, the Orsang man can be seen as the oldest *Homo sapiens* of the subcontinent.

Introduction

Hominin occupation in the Indian subcontinent by the middle Pleistocene was widespread as confirmed by substantial archaeological evidences from south Asia (Mishra et al., 1995; Petraglia, 2001; Paddayya et al., 2002) and origin of Anatomically Modern Human (AMH) in the mainland Asia (Wolpoff et al. 1984) is again in debate (Coppens et al., 2008; Dambricourt Malassé 2009, 2013; Wu et al., 2010; Chamyal et al., 2011; Sankhyan et al., 2012; Demeter et al., 2012). The details of the human calvarium discovered in Gujarat from the Quaternary alluvial sediments of Orsang river, at Ratanpur in the lower Narmada basin, have been reported by Chamyal et al (2011). Infra-red stimulated luminescence (IRSL) dating was carried out on coarse grained feldspar extracted from the host sediments and those within the skull and the results were considered as the minimum ages. The host sediments at the same level as that of the skull gave an age of 38±5 ka and 45±7 ka. The sediments inside the skull yielded an age of 30±7 ka and 27±4 ka, suggesting, that the exposed sediment sequence at Ratanpur was deposited during the upper part of late Pleistocene. ^{14}C dating of the skull using AMS method provided an age of 4600 ± 200 ka B.P. The skull was identified as *Homo sapiens* with features which threw new light on the biological relationships between Asian *Homo erectus* and Early Asian *Homo sapiens*. The Orsang calvarium was compared with 130 skulls from lower to late Pleistocene (collection of the Institute of Human Paleontology, Paris) and its age debated. In continuation with the previous study by Chamyal et al (2011), Beck et al (2012) have undertaken micro CT reconstruction (X ray microtomography) and Ion Beam Analysis (IBA) to check the preservation of bone structure and to understand the diagenetic alteration of the bone tissue. This article analyses the computed tomography (CT scan) of the skull which supports the hypothesis of a quick burying of the body in the late Pleistocene sediments and establishes that in the absence of new contradictory data, the Orsang man can be seen as the oldest *Homo sapiens* of the subcontinent.

Diagenetic alteration of bone tissues

Initially the first sample of bone studied for dating was taken on the part damaged by exposure to the air. This exposure has probably accelerated the process of degradation of collagen and biased radiocarbon dates. A second sample was taken from a skull part protected by the sediments in order to check the structural preservation of the bone. A piece from the left orbital cavity was made available for investigations on fine-scale structure. A high resolution micro-CT (X-ray microtomography) reconstruction of the bone sample was obtained at the Natural History Museum of London using a Nikon Metrology HMXST CT System. Compared to corresponding recent human bone, the fossil shows increased normal porosity with some internal deposits of sedimentary origin. In an another study, a new experimental protocol have been carried out for chemical composition measurements of Orsang and of the skull from the rockshelter Abri Pataud (Late Upper Paleolithic, Dordogne, France) by using the external proton micro-beam of AGLAE (The Centre for Research and Restoration of the Museums of France, C2RMF-Paris) applied simultaneously with PIXE (particle induced x-ray emission) and RBS (Rutherford backscattering) in order to assess the collagen content. By using 3 MeV protons, the PIXE spectra give access to the determination of element Na to U, and backscattering spectrometry is well adapted for the quantification of carbon, nitrogen and oxygen. To validate the procedure, nuclear reactions have been undertaken at the JANNUS laboratory (CEA-Saclay, France) with a 2 MeV Van de Graff accelerator. Carbon, nitrogen and oxygen concentrations have been measured. The results showed a rate of preservation sufficient for a new ^{14}C dating of the skull with this sample (Beck et al. 2012).

The skull, morphology

The morphological characters were studied at the M. S. University of Baroda, while most part of comparative anatomy was done at the Department of Prehistory, National Museum of Natural History, with the anthropological collection of the Institute of Human Paleontology (IPH), Paris. The CT scan was realized in 2011 by Dr. S. Shah, Aster Diagnostic & Therapeutic Radiology Services, Vadodara. The analyses in Paris allow comparative anatomy, and measurements were verified directly on the scan.

The skull was partially emptied of its fill in the laboratory. A first observation of the sediment shows a stratification attesting to a quiet hydraulic regime and its horizontal orientation indicates that the body was on the back with the head inclined on the right side (Fig. 1A, B, C). The preservation of fragile parts i.e. the root of the styloid apophysis visible on the right side, the clivus in connexion with the petrous pyramid, the occipital condyles, the auditory canal and the temporo-mandibular joints, indicate that no displacement of the skull occurred since its quick burial.

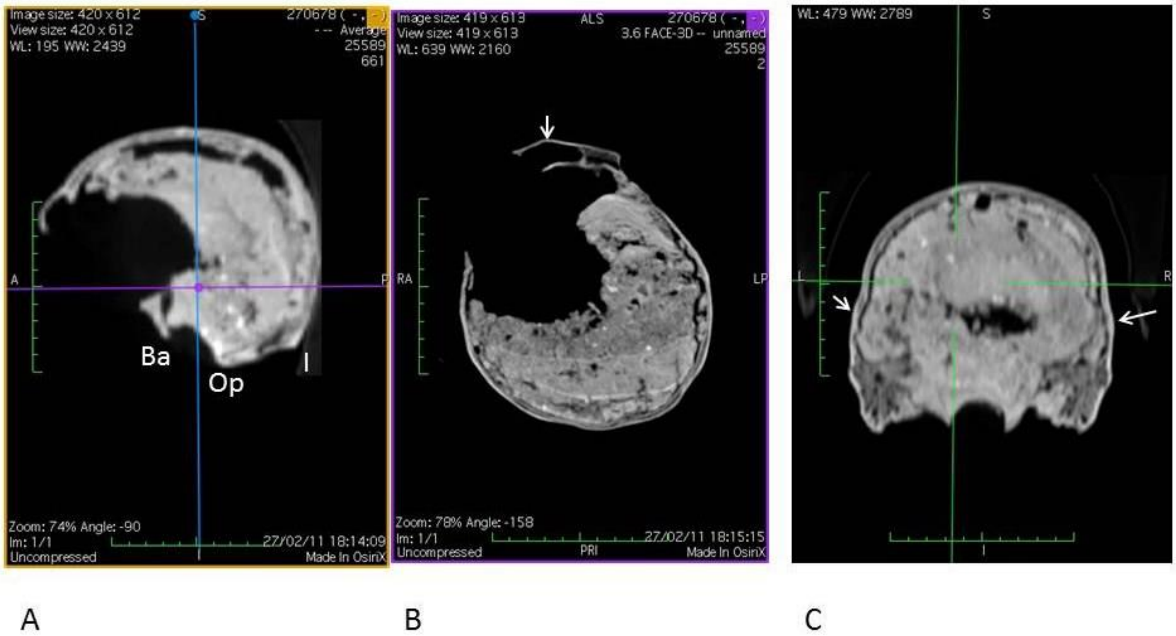

Fig 1 CT scan of Orsang calvarium. A: midsagittal section with Ba basion, Op opisthion, I: inion. The clivus is visible. B longitudinal section showing the broad frontal sinus (arrow) and the stratification of the sediments, C: coronal section in the posterior part of the calvarium with the two temporal bosses (white arrows). CT scan, Dr. S. Shah. © A. Dambricourt Malassé.

The two mastoid processes are quite well developed and support the calvarium when it is placed on a horizontal surface, this argues in favour of a male individual. The degree of synostosis of the cranial sutures is high, the lambdoid and sagittal sutures attesting a mature adult stage. Besides these, other features worth noting are the remarkable anatomical characteristics. A very broad frontal sinus of 16 mm is visible between the inner and outer compact tables in the glabellar area without supra-glabellar depression; the pneumatization of the frontal sinus extended laterally on 174 mm, the external orbital apophysis not concerned is gracile (Fig. 1B and Fig. 2A, B, C). On the superior part of the vault there are a post-bregmatic depression and an important ossification of the coronal synostosis visible only with the CT scan indicating a coronal craniostenosis. The trace of a metopic suture is visible. The nuchal plane and the exocranial surface of the cerebellar fossa is short, and above them the supra-iniac zone is flat and vertical; the profile presents an important planoccipitaly; there is no *torus occipitalis*, nevertheless the external occipital protuberance (inion) and the superior nuchal line are developed. Muscular aponeuroses are well distinct on the left side of the cranium, especially those of the temporal muscle elongated vertically and rough, and those of the posterior belly of the digastric muscle. The right side does not show these features. This asymmetry could be compared to the one seen in inferior and superior views. A very well-developed asteriac process forms a thickening of the outer compact bone in the *pars asterica* of the parietal squama (Fig. 2B). Two vascular orifices delimit the relief which tends to overhang the occipital bone and can be defined as a gracile *torus angularis*. In *Homo erectus*, this protuberance is more developed in continuity with a marked superior temporal line which is not visible on the Orsang skull. In the approximate Frankfurt plane, its position is at the level of the zygomatic process and not above as in *Homo erectus narmadensis*, because of the downward and forward growth of the cerebellar fossa, which is very specific of the evolutionary grade of Anatomically Modern Human (AMH). The maximal width is in the lower part of the skull as in *Homo erectus* but two characters must be distinguished, i) a bulging of the temporal squama never seen in the normal growth of AMH (Fig. 1C) and ii) a well-developed supramastoidian temporal crest protuberance on a pneumatised petrous bone (Fig. 2C). In posterior view, the mastoid processes are not in a vertical alignment with the parietal eminences, a *Homo sapiens* conformation; they adopt an inclination resulting from this enlargement caused by both exocranial (crest) and endocranial (bulging) developments of the temporal squama. The glenoïd fossa of the temporal is better protected than the right one, which was exposed to air; they are asymmetrical, the left being appreciably wider and deeper. They are large-sized.

Fig. 2 A: the sinus frontal in the glabellar area, B: CT scan showing the strong coronal synostosis and the trace of a metopic suture (arrows), C: the left parietal and temporal bone with a: temporal bosse, b: supramastoidian crest, c: *torus angularis*. (CT scan, Dr. S. Shah). © A. Dambricourt Malassé.

Biometry

Since several parts are missing to apply Martin and Seller measures, remarkable distances were taken with homologous anatomical points to be reproducible on other skull series. One measurement based on the CT scan is changing with the basi-bregmatic height; 126 mm and not 132 mm that modifies the cranial capacity estimation and the height/length ratio (Table 1). The maximum length (glabella-opisthocranion) is 170 mm. According to Martin and Seller, when symmetrical lateral expansion is excessive, euryon does not be located on the entire adjacent region above the external auditory meatus. Nevertheless with

Orsang skull, the case is particular because the planoccipitaly can be correlated to a lateral expansion of the neurocranial cavity as seen below. Both cases have been taken into account, euryon on parietal and temporal squama. The greatest breadth is bitemporal, between the crests (146 mm), but also between the temporal bosses (145 mm), the horizontal cephalic index classifies the skull in the category of hyperbrachycranium. The ratio between the maximum height (basion-bregma, 126 mm) and the bitemporal squama (145 mm) accentuates the broad aspect of the skull (86, 03). Finally the height / length ratio shows a sharply longer skull (170 mm) than high (126 mm). The cranial capacity is estimated based on the exocranial measures according to the Martin's equation: 0.00037 (length x width (euryon-euryon) x basion-bregma height) + 328± 73. If the distance between the two euryons is located on the parietal bones, the capacity is 1342 ml. But the CT scan shows clearly that the distance between the two temporal bosses are greater than between the parietals. The estimation of the cranial capacity is 1485 ml. The *foramen magnum* is asymmetrical and wide (index = 85,7).

CT scan analysis and interpretation

The bones of the vault are of membranous formation, this conformation result from a combination of neural and hormonal growths. The maximum length (glabella-opisthocranion) corresponds to *Homo erectus s. l.* but the values do not reflect growth homologies isolated from the morphogenetic trajectories. It is clear that the forward and downward development of the cerebellum is typically that of AMH. Whatever the cranial capacity, the posterior cranial fossa morphogenesis can never be confused with that of the oldest species defining the Homo grade (*Homo georgicus*, *Homo habilis*, *Homo erectus*) visible with their late evolved relatives such as *Homo neanderthalensis* in Western Europe and *Homo floresiensis* in Indonesia (Dambricourt Malassé 2011). The study of the skull base growth takes into consideration the flexion of the spheno-occipital synchondrosis, a very important factor in cranio-facial orthopaedic such as orthodontics (Maestripieri et al., 2002), in cranio-sacral therapy and osteopathy (Cook 2005, Downey et al. 2010). When the flexion is too active, it brings the clivus and the *tentorium cerebelli* forward and downward and hence limits the backward growth of the occipital squama. The maximal length tends to reduce so that the opisthocranion can merge to the inion resulting in planoccipitaly. The mid-sagittal section of the CT scan confirms a straightening of the sphenobasilar slope (clivus) and a short posterior fossa (Fig 1A). CT scan has revealed the distance between the two temporal endocranial tables just above the petrous pyramid, is enlarged and a possible consequence of the impossibility for the brain to growth posteriorly.

The hyperbrachycephaly conformation can be seen as the result of a neural growth and specific suture activities with a great flexion of the spheno-occipital synchondrosis, a shortening of the cerebellar fossa, early ossification of the coronal and quick synostosis of the lambdoïd sutures. This skull is not a strong case of craniostenoses, but the convergence with such abnormalities reveals congenital factors in favour of endemism.

The Asian regionalisation of the *torus angularis* (Dambricourt Malassé 2008, 2011, Chamyal et al. 2011) suggests that some populations were isolated from genetic flows coming from Africa, Near East and Europe, which mean that endemism played an important role for the differentiation of geographical diversities during at least 1.8 million years as shown by late *Homo florensiensis* in Indonesia (c.a. 18 ka). Only one African Pleistocene skull developed a *torus angularis*, Kabwe (*Homo rhodensiensis*, Middle Pleistocene) which supports evidences of a geographical arch of Asian-Arabo-African gene flows at that time.

For living populations the *torus angularis* (or *process asteriacus* in modern man), is still visible in certain Mongoloïd and Australoïd populations with high incidence of other bone thickenings like retromastoid process and supramastoid tubercle.

Discussion and conclusion

The time gap between late evolved *Homo erectus* and Anatomically Modern Human, or *Homo sapiens Linnaeus*, has been filled recently with the discovery of the Chongzuo mandible (Zhiren cave) in South China dated of 110 ka (Liu et al. 2010). Contrary to critics questioning the possibility of a parallel emergence of modern anatomy in Asia, the release of the *trigonum mentale* under the incisor dental arch that shapes the first appearance of the *mentum osseum* is never visible on *H. habilis*, *H. erectus*, *H. georgicus*, *H. antecessor*, *H. heidelbergensis*, and on the late *Homo neanderthalensis* and *Homo floresiensis*. The oldest *mentum osseum* known before the Chinese discovery is Omo Kibish 1 (Ethiopia 200 ka) then Qafzeh (Near East 95 ka, for instance Qafzeh 7 original mandible at IPH).

The Pleistocene Anatomically Modern Human developed cranial capacity around 1400-1600 ml, for instance as in Iberomaurusian people greater than in Holocene people, but the brachycephaly is not visible before Mesolithic i.e. 9000 ka BP. Orsang cranial capacity (1485 ml) corresponds to the Paleolithic peoples, while its hyperbrachycranial conformation results of neural growth abnormalities. With its conspicuously developed glabellar pneumatization, its well-marked post-cranial superstructures, the skull from Orsang valley is closer to the robust *Homo sapiens* of the late Pleistocene than to the gracile Neolithic populations. Besides, with its well-developed *torus angularis*, this skull attests to the presence of Asian *Homo erectus* genes in its hereditary material and allows concluding that among ancestors of Orsang valleys populations were late Asian *Homo erectus* living in the Narmada basin, such as the large brained *Homo erectus narmadensis*. The paradigm of replacement by African anatomically modern humans arriving in Asia around 90 – 70 ka and extinction of autochthonous populations can no more be supported by recent paleontological data, the mandible of Chongzuo in South China dated of 110 ka and the Late Pleistocene skull of Orsang in Central India, with early Eurasian feature, the *torus angularis*.

References

Beck L, Cuif JP, Pichon L, Vaubaillon S, Dambricourt Malassé A, Abel RL. 2012. Checking collagen preservation in archaeological bone by non-destructive studies (Micro-CT and IBA). Original Research Article. Nuclear Instruments and Methods in Physics Research Section B: Beam Interactions with Materials and Atoms, 273: 203-207. ISSN: 0168-583X.

Chamyal L, Dambricourt Malassé A, Maurya DM, Raj R, Bandhari S, Pant SK, Gaillard C. 2011. Discovery of a robust Homo sapiens in India (Orsang, Lower Narmada Basin, Gujrat). Possible continuity with Indian Homo erectus. Acta Anthropologia Sinica, 2: 167-191.

Cook A. 2005. The Sphenobasilar Synchnodrosis (SBS) Revisited - The Mechanics of Cranial Motion. Journal of Bodywork and Movement Therapies, 9, 3: 177-188.

Coppens Y, Tseveendorj D, Demeter F, Turbat T, Giscard PH. 2008. Discovery of an archaic Homo sapiens skullcap in Northeast Mongolia Comptes Rendus Palevol,7, 1: 51-60.

Dambricourt Malassé A. 2009. Embryogeny and Human phylogeny. Chapitre 8. In: A.R. Sankhyan Asian Perspectives on Human Evolution, New Delhi. Ed Serial Publications. 103-121.

Dambricourt Malassé A. 2011. Permanent bipedal equilibrium, embryonic origin, morphogenesis, occlusal-postural balance, impact on psychomotor and behavioral of hominid evolution (in French). Accreditation to Direct Research, 706 p.

Dambricourt Malassé A. 2013. The emergence of gracile human anatomy during the Holocene in Asia: convergent acclimation and\or phylogenetic trend? The example of the occlusion. In: B.H. Kotlia, Holocene: Perspectives, Environmental Dynamics and Impact Events, Nova Sciences Publishers Inc. (Ed), New-York.

Demeter F, Shackelford L, Bacon AM, Duringer P, Westaway K, Sayavongkhamdy T, Braga J, Sichanthongtip P, Khamdalavong P, Ponche JL, Wang H, Lundstrom C, Patole-Edoumba E, Karpoff AM. 2012. Anatomically modern human in Southeast Asia (Laos) by 46 ka, Proc. Natl. Acad. Sci. U. S. A., 109, 36:14375-14380.

Downey P.A, Barbano T, Kapur-Wadhwa R, Sciote JJ, Siegel MI, Mooney MP. 2010. Craniosacral therapy: the effects of cranial manipulation on intracranial pressure and cranial bone movement. Journal of Orthopaedic and Sport Physical Therapy: 845-853.

Liu W, Jin C, Zhang YQ, Cai YJ, Xing S, Wu XJ, Cheng H, Edwards RL, Pan WS, Qin DG, An ZS, Trinkaus E, Wu XZ. 2010. Human remains from Zhirendong, South China, and modern human emergence in East Asia. Proceedings of the National Academy of Sciences, Proc. Natl. Acad. Sci. U. S. A., 107, 45: 19201-19206.

Mishra, S., Venkatesan, T.R., Rajaguru, S.N., Somayajulu, B.L.K., 1995. Earliest Acheulian industry from peninsular India. Current Anthropology 36, 847–851.

Paddayya, K., Blackwell, B.A.B., Jhaldiyal, R., Petraglia, M., Fevrier, S., Chaderton, D.A.I., 2002. Recent findings on the Acheulian of the Hunsgi and Baichbal Valleys, Karnataka, with special reference to the Isampur excavation and its dating. Current Science 83, 641–647.

Petraglia, M., 2001. The Lower Palaeolithic of India and its behavioural significance. In: Barham, L., Robson-Brown, K. (Eds.), Human Roots: Africa and Asia in the Middle Pleistocene. Western Academic and Specialist Press, Bristol : 217–233.

Sankhyan A, Badam G, Dewangan L, Chakraborty S, Prabha S, Kundu S, Chakravarty R. 2012. New Postcranial Hominin Fossils from the Central Narmada Valley, India, Advances in Anthropology, 2, 3: 125-131.

Wolpoff MH, Wu XZ, Thorne AG. 1984. Modern Homo sapiens Origins: A General Theory of Hominid Evolution Involving the Fossil Evidence from East Asia. In: The Origins of Modern Humans: A World Survey of the Fossil Evidence, eds. F.H. Smith and F. Spencer. Liss, New York: 411-483.

Table 1 Orsang skull measurements in millimeters (number in the left column correspond to Martin and Saller 1956)

ORSANG Cranium	Notes
1 maximum length glabella-opisthocranion	170 inion and opisthocranion coinciding
8 maximum breadth	146 location: supramastoid crest
bi-temporal breadth	145 between the two temporal bosses
bi-parietal breadth	128 between the two parietal bosses
17 basi-bregmatic height	126 CT scan measure
20 auriculo-bregmatic height	105
horizontal cranial index temporal 100xl/L parietal 100xl/L	 85.88 hyperbrachycranium 75. 29 mesocranium
index of height/length auriculo-bregmatic height/ max. cranial length basi-bregmatic height/ max. cranial length index of height/breadth auriculo-bregmatic height/ max. cranial breadth basi-bregmatic height/ max. cranial breadth	 61.76 orthocranium (low vault) 74.11 low skull 71.91 wide vault 86.30 wide vault
cranial capacity maximum breadth bi-parietal breadth	 1485 ml +- 73
frontal sagittal curvature 26 nasion-bregma arc 29 nasion-bregma chord index	 116 104 89.65
divergence of the frontal 9 minimum frontal breadth 10 maximum frontal breadth index of divergence	 110 by symmetry 112,5 97.77
nasion-inion arc	297
Parietal : length of sagittal arc/temporal arc 27 Sagittal arc of parietal arc of parietal with temporal edge curvature index	 122 105 116.19 high index probably caused by the planoccipitaly
Upper temporal line to temporal edge	37 (between the highest point of

	the superior temporal curve and the highest point of the superior temporal line)
stephanion-bregma chord	superior stephanion: 60 mm inferior stephanion: 67 mm
upper stephanion arc	112
upper stephanion chord	103
nasion-frontomalar suture	47 (in horizontal plane)
45 bizygomatic breadth	128 anterior zygomatic tubercle
bi-asterion breadth	109
11 bi-porion breadth	132
bi-pterion breadth	100
bi-mastoid breadth	106
porion-asterion length	left : 45 right : 44
Length between the summit of the mastoid process and the centre of the carotid canal	28
Foramen magnum 7 length width index	 35 30 85.71 wide foramen magnum